Response modality-dependent abstract choice representations for vibrotactile comparisons

Yuan-hao Wu [a], Lisa A. Velenosi [b], and Felix Blankenburg [a, b]

[a] Neurocomputation and Neuroimaging Unit (NNU), Department of Education and Psychology, Freie Universität Berlin, Habelschwerdter Allee 45, 14195 Berlin, Germany

[b] Bernstein Center for Computational Neuroscience Berlin, Humboldt-Universität zu Berlin, Unter den Linden, 10099 Berlin, Germany

Corresponding Author:

Yuan-hao Wu

Freie Universität Berlin

Department of Education and Psychology

Neurocomputation and Neuroimaging Unit (NNU)

Habelschwerdter Allee 45 14195 Berlin

yuan-hao.wu@fu-berlin.de

Abstract

Previous electrophysiological studies in monkeys and humans suggest that premotor regions are the primary loci for the encoding of perceptual choices during vibrotactile comparisons. However, these studies employed paradigms wherein choices were inextricably linked with the physical properties of the stimuli and action selection. It raises the question what brain regions represent choices at a more abstract level, independent of the sensorimotor components of the task. To address this question, we used fMRI-MVPA and a variant of the vibrotactile frequency discrimination task which enabled the isolation of choice-related signals from those related to stimulus properties and selection of the manual decision reports. We identified the left, contralateral dorsal premotor cortex (PMd) and intraparietal sulcus (IPS) as carrying information about abstract choices. Notably, our previous work using an oculomotor variant of the task also reported abstract choice representation in intraparietal and premotor regions. However, the informative premotor cluster was centered in the frontal eye fields rather than in the PMd, providing empirical support for a response effector-dependent organization of abstract choice representation in the context of vibrotactile comparisons. Considering our results together with findings from recent studies in animals, we speculate that the premotor region likely serves as a temporary storage site for information necessary for the specification of concrete manual movements, while the IPS might be more directly involved in the computation of choice.

Keywords

Vibrotactile comparison, perceptual decision making, categorical choice, fMRI, multivariate pattern analysis

Introduction

In everyday life, we are continuously encountering situations wherein we need to make decisions based on comparisons between stimuli occurring at different times. Imagine choosing an avocado at a grocery store: one squeezes two or more avocados sequentially and decides for one based on their firmness. The neural processes underlying this type of decision have been extensively studied in the somatosensory domain using the vibrotactile frequency discrimination task (reviewed in Romo & de Lafuente, 2013). In their seminal work, Romo and colleagues trained monkeys to compare frequencies of two sequentially presented vibrotactile stimuli and report with a manual response whether the second frequency (f2) was higher or lower than the first (f1). Crucially, firing rates in premotor regions implicated in the planning and execution of manual movements, such as the supplementary motor area (SMA), ventral (PMv), and dorsal premotor cortices (PMd), have been consistently found to reflect perceptual choices (Hernández et al., 2002, 2010; Romo et al., 2004).

The involvement of motor-related regions during vibrotactile comparisons also agrees well with findings from an influential line of decision-making research in the visual domain. Monkey neurophysiological experiments employing random motion dot tasks with saccade responses consistently reported decision-related signals in regions implicated in saccadic movement (reviewed in Gold & Shadlen, 2007), such as the lateral intraparietal area (LIP, Shadlen & Newsome, 2001; Roitman & Shadlen, 2002), the frontal eye fields (FEF, Kim & Shadlen, 1999; Ding & Gold, 2012), and the superior colliculus (Horwitz & Newsome, 1999; Ratcliff et al., 2003). Findings from these two lines of work have converged to the view that decisions are directly implemented in regions involved in the planning and execution of the resultant action

(Gold & Shadlen, 2007; Cisek & Kalaska, 2010). In other words, decisions are implemented in a response modality-dependent manner. Moreover, the posited response modality-specific implementation appears to translate to human vibrotactile comparisons. Herding and colleagues (2016, 2017) reported premotor regions as the most likely source of choice-selective beta oscillatory activity in the EEG signal. The choice-related modulation was localized in the medial part of the premotor cortex when human observers used button presses to indicate their choices (Herding et al., 2016). However, when they reported their choices with saccades, the source of the choice-related modulation shifted to the FEF (Herding et al., 2017).

Of importance, the majority of findings in the context of vibrotactile comparisons were yielded from experimental settings wherein perceptual choices were inextricably linked to the sensory and motor components of the task. In such settings, f1 typically serves as the reference stimulus against which f2 (the comparison stimulus) is compared. Thus, observers will mostly decide for the percept “higher” if frequencies were presented in an increasing order (f1 < f2), and “lower” if presented in a decreasing order (f1 < f2). The abstract contents of perceptual choices are directly bound with the physical properties of the stimulus presentation. Moreover, decisions are typically implemented as choices between two hand or saccade movements so that choosing a particular percept is the same as choosing a specific hand or saccade movement. Due to these dependencies, the presumed choice-related signals may reflect a multiplicity of choice and sensorimotor aspects, rather than the choice per se (Park et al, 2014, see also Huk et al., 2016 for a review). This limitation leaves open the question of whether choices are represented in a more abstract, internal cognitive format, uncontaminated by stimulus order and action selection. For

93 succinctness, we refer to this more abstract type of choice representation as an
94 abstract choice representation throughout the rest of this article.

95 Our previous work (Wu et al., 2019) addressed this question by means of human
96 fMRI-MVPA and a novel variant of the vibrotactile frequency discrimination task.
97 Intriguingly, although participants' choices were decoupled from the preceding
98 stimulus orders and ensuing saccade movements used for reporting the decisions,
99 regions implicated in saccade planning and selection such as the FEF and
100 intraparietal sulci (IPS) were identified as representing abstract choices. The finding
101 suggests that activities in these human brain regions are not confined to the sensory
102 and motor aspects of perceptual decisions, but involved in more abstract cognitive
103 computation. Moreover, it hints at the possibility that abstract choices may also be
104 represented in an effector-specific manner.

105 In the present fMRI study, we sought to further explore the interplay between the
106 topographic organization of abstract choice representations and response modality
107 during vibrotactile comparisons. We asked participants to perform an analogous
108 version of the vibrotactile frequency discrimination task as in our previous work, with
109 saccade responses replaced by manual button presses. Further, the same whole-
110 brain searchlight multivariate analysis routines (Kriegeskorte et al., 2006) as
111 implemented in the previous work was employed to identify brain regions that carry
112 information about abstract choices. Following the interpretation drawn from our
113 previous study, we expected abstract choice representations in premotor regions
114 implicated in the selection of manual responses such as the PMd, PMv, or SMA.

115

Materials and methods

Participants

Thirty-one volunteers participated in the fMRI experiment. They were right-handed, had no history of neurological or psychiatric impairment, and normal or corrected-to-normal vision. Data of four participants were excluded due to poor behavioral performance (accuracy rate < 0.5 in at least one stimulus pair), leaving the data of 27 participants in the analyses (18 females and 9 males; mean age: 25, range: 18–34). All participants provided written informed consent as approved by the ethics committee of the Freie Universität Berlin and received monetary compensation for their time.

Task design and stimuli

We asked participants to complete a variant of the vibrotactile frequency discrimination task (Fig. 1). Similar to standard versions of the task, participants compared two sequentially presented vibrotactile frequencies and made a decision on whether the frequency of the comparison stimulus was higher or lower than that of the reference stimulus. It differed from standard versions in two important aspects: First, we introduced task rules that alternately designate f1 or f2 as the comparison/reference stimulus across trials so that the perceptual choices were independent of the physical properties of the stimulus order. Second, instead of using a direct choice-motor response mapping, participants reported a match or mismatch between their percept and the proposition of a visual matching cue. After the decision phase, participants selected a color-coded target after a decision phase, from which their perceptual choice was inferred. Hence, participants were not able to plan a

specific manual movement or anticipate a target color during the decision phase. As a consequence of these measures, if there were detectable choice-related signals during the decision phase, it would be unlikely to result from the physical properties of the stimulus order or action selection.

Each trial was preceded by a variable fixation period (3 – 6 s), during which participants were asked to fixate on a gray cross centrally presented on the screen. The trial started with a switch from the fixation cross to either a square or a diamond for 500 ms, instructing participants which task rule applies in the current trial. In half of the trials, participants used f1 as the comparison stimulus and evaluated whether it was higher or lower than the reference stimulus f2. In the other half, participants made comparisons in the reversed direction. That is, they evaluated f2 relative to f1. The rule cue was followed by two sequentially presented vibrotactile stimuli with different frequencies administered to participants' left index finger (each of 500 ms separated by a 1 s retention). After a decision phase of 2 s, a visual matching cue in the form of either an upward-pointing or a downward-pointing equilateral triangle appeared centrally on the screen for 500 ms, indicating a comparison stimulus of higher or lower frequency, respectively. Following the offset of the visual matching cue, a target screen with a central fixation cross and two color-coded targets (blue and yellow disks) in the periphery along the horizontal meridian was displayed for 1.5 s. During this time period, participants reported a match or mismatch between their perceptual choice ('higher' vs. 'lower') and the visual matching cue by selecting one of the color-coded targets corresponding to their report. Depending on the spatial location of the corresponding target, participants pressed the left or right button of a response box held in their right hand with their index or middle finger.

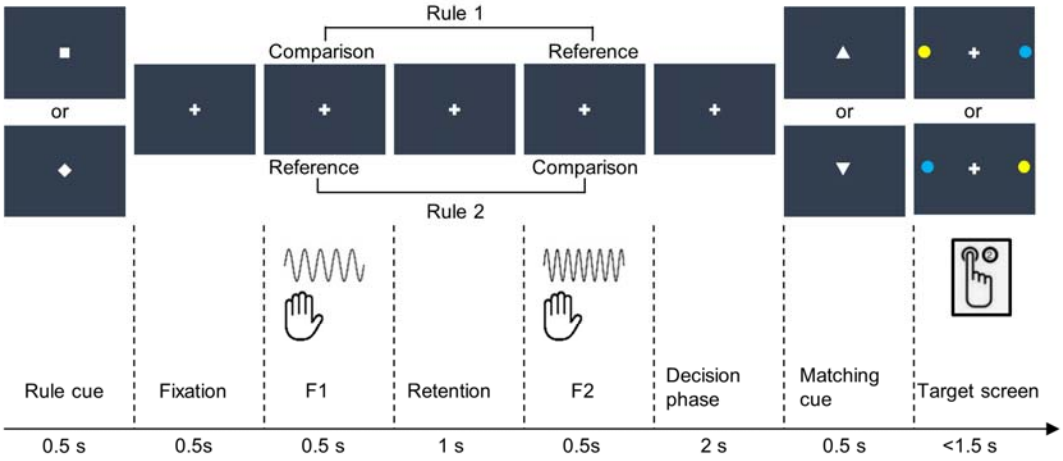

Fig. 1. Trial schematic. A rule cue (square or diamond) indicated whether f1 or f2 served as the comparison stimulus. The stimuli presentation was followed by a decision phase. Thereafter, a matching cue (equilateral triangle) was presented. An upward-pointing triangle represented a comparison stimulus of higher frequency, while a downward-pointing triangle represented a lower comparison frequency. Participants compared their perceptual choice with the matching cue. A match or mismatch was indicated by choosing one of the color-coded disks presented in the periphery via a button press. See Wu et al. (2019) for an oculomotor variant of the task.

Visual stimuli were generated using MATLAB version 8.2 (The MathWorks, Inc, Natick, MA) and the Psychophysics toolbox version 3 (Brainard, 1997). Except for the two peripheral, color-coded discs on target screens, all other visual symbols were presented centrally in white on a black background. During the fMRI session, visual stimuli were projected with an LCD projector (800 x 600, 60 Hz frame rate) onto a screen on the MR scanner's bore opening. Participants observed the visual stimuli via a mirror attached to the MR head coil from a distance of 110 ± 2 cm. Suprathreshold vibrotactile stimuli with a consistent peak amplitude were applied to participants' distal phalanx of the left index finger using a 16-dot piezoelectric Braille-like display (4 x 4 quadratic matrix, 2.5 mm spacing), controlled by a programmable stimulator (QuaeroSys Medical Devices, Schotten, Germany). Frequencies of the first vibratory stimuli (f1) varied between16 and 28 Hz in steps of 4 Hz. The second

185 stimulus was either 4 Hz higher or lower than the preceding f1, yielding a total of
186 eight possible stimulus pairs.

187 Participants performed six experimental runs of the vibrotactile frequency
188 discrimination task, each lasting ~12.5 min. During each run, each stimulus pair was
189 presented eight times, each time with a unique combination between rule cues
190 (diamond vs. square), matching cues (upward-pointing vs. downward-pointing
191 triangles), and target screens (blue-left, yellow-right vs. yellow-left, blue-right). This
192 yielded a total of 64 trials per run, which were presented in a randomized order.
193 Further, the association between visual symbols and task rules as well as between
194 target colors and match reports was counterbalanced across participants.

195

196 **FMRI data acquisition**

197 The fMRI data were obtained with a 3 T Tim Trio MRI scanner (Siemens, Erlangen,
198 Germany) equipped with a 12-channel head coil at the Center for Cognitive
199 Neuroscience Berlin. Functional volumes sensitive to the BOLD signal were acquired
200 using a T2* weighted echo planar imaging sequence (TR = 2000 ms, TE = 30 ms,
201 field of view = 192 mm, flip angle = 70°). Each volume consisted of 37 axial slices
202 and was acquired in an interleaved order (64x64 in-plane, 3 mm isotropic with 0.6
203 mm gaps between slices). 378 functional volumes were obtained in each
204 experimental run. In addition to the six experimental runs, a T1 weighted structural
205 volume was acquired for co-registration and spatial normalization purposes using a
206 3D MPRAGE sequence (TR = 1900 ms, TE = 2.52 ms, 256x256 in-plane, 1mm
207 isotropic).

208

Data preprocessing and analyses

FMRI data preprocessing and general linear model (GLM) were performed with SPM12 version 6685 (www.fil.ion.ucl.ac.uk/spm) and custom MATLAB scripts (https://github.com/yuanhaowu/DecodingAbstractChoices), while multivariate decoding analyses were performed using The Decoding Toolbox version 3.991 (Hebart et al. 2017, https://sites.google.com/site/tdtdecodingtoolbox/). During the preprocessing, functional volumes were corrected for slice acquisition time differences and spatially realigned to the mean functional volume.

Decoding choices. The focus of the present study was to identify brain regions that carry information about choice-related information independent of stimulus order and selection of specific manual response. To this end, we used MVPA combined with a whole-brain searchlight routine to pinpoint brain regions that show distinguishable local activity patterns between different choices during the decision phase.

We first obtained run-wise beta estimates for choice-related activity during the decision phase for each voxel. We fitted a GLM (192 s high-pass filter) to each participant's data. Separate impulse regressors were defined to model the two choices ('higher' vs. 'lower'), convolved with the canonical hemodynamic function at the onsets of the decision phases. To minimize the number of potential indecisions during decision phases, only correctly answered trials were modelled. Incorrectly answered and missed trials were modelled with a separate regressor of non-interest and not included in the subsequent MVPA. In addition, six movement parameters, the first five principal components explaining variance in the white matter and cerebrospinal fluid signals respectively (Behzadi et al., 2007), and a run constant were added as nuisance regressors, culminating in a total of 120 parameter estimates per participant (20 x 6 runs).

To identify brain regions that exhibit choice-selective activity patterns, a searchlight MVPA was performed on each participant's data using linear support vector machine classifiers (SVM) in the implementation of LIBSVM 2.86 (Chang & Lin, 2011) with a fixed cost parameter of c = 1. We generated a 4 voxel radius spherical searchlight and moved it voxel-by-voxel through the entire measured volume. The searchlight was centered on each voxel in turn and comprised a maximum of 251 voxels (note that searchlights with 3 and 5 voxel radii yielded similar results). At each voxel, run-wise beta estimates for each of the two choice regressors extracted from voxels within the searchlight formed the 12 response patterns (2 conditions x 6 runs) for the decoding analysis. To avoid overfitting, we estimated the classifier's decoding accuracy using a leave-one-run-out cross-validation routine. That is, we iteratively trained the classifier to distinguish between response patterns between participant's choices with data from five runs and tested how well the classifier predicted participant's choices based on response patterns in the remaining run. This procedure was repeated until all runs were used as the test set. The decoding accuracy of the classifier was estimated as the number of correct predictions divided by the number of all predictions. Decoding accuracy resulting from the searchlight analysis around a given voxel was stored to the corresponding location of a whole-brain volume before the searchlight moved to the next voxel. The searchlight analysis was applied to all voxels in the measured volume so that a continuous whole-brain accuracy map could be obtained. For each voxel in the measured volume, the resulting accuracy map displayed the extent to which the multivariate signal in the local spherical neighborhood was selective to choices. Notably, due to the use of a balanced design, different perceptual choices were expected to have approximately the same number of trials associated with each stimulus order and motor response. That is, each choice regressor contained roughly the same amount of information

about stimulus order and button press. Thus, choice-selective activity detected during the decision phase would be unlikely to result from the physical properties of stimulus order or planning of button press responses.

For the group inference, each participant's accuracy map was transformed to MNI space, resampled to 2 x 2 x 2 mm^3 voxel size, and smoothed with a 3mm full width at half maximum Gaussian filter. The transformed maps were submitted to a group one-tailed, one-sample t-test to assess whether the decoding accuracy at any voxel was significantly higher than the chance level (50%). A voxel with significant above-chance decoding accuracy would indicate that the local activity pattern around that voxel carries information about choices.

Behavioral control analyses. By virtue of the balanced experimental design, the implemented variant of the vibrotactile frequency discrimination task has proven to be capable of disentangling choice-related activity from that related to sensory and motor task components (Wu et al., 2019). However, it remains possible that the classifier could exploit the subtle difference in the distributions of the two stimulus orders (f1 > f2 vs f1 < f1) or motor responses (left vs right button press) between choice conditions to achieve above-chance decoding accuracy (Görgen et al., 2018; Hebart & Baker, 2018). This is of particular relevance for the present study as the balanced number of trials across conditions might not hold after the exclusion of incorrect answered trials and have a biasing effect on MVPA on fMRI data. To address this concern, we applied the same decoding analysis pipeline used with to behavioral data, which enabled us to directly test whether choices can be predicted based on the number of trials associated with different stimulus orders and motor responses in each choice.

For each of the variables of interest, we performed an independent analysis with the following procedure: For each choice in each run, we generated a two-dimensional vector using the number of trials associated with different variable levels. For instance, if a participant responded 15 times with a left and 17 times with a right button press to indicate a comparison stimulus of higher frequency, it was coded as [15 17]. The remainder of the analysis proceeded in a manner analogous to the fMRI data analysis pipeline. Twelve data vectors (2 choices x 6 runs) were used to predict participant's choices in a decoding analysis with a leave-one-run-out cross-validation routine. For the group inference, we used one-tailed Wilcoxon sign rank tests to probe the statistical significance against chance accuracy (50%). Significant results would imply potential confounds due to the biased distributions of stimulus orders or/and motor responses.

Neuroimaging control analysis. As informative clusters identified in the main fMRI analysis include brain regions typically implicated in the planning and execution of manual movements (see result), we did an additional analysis on fMRI data to test whether the result might be confounded with motor planning. We repeated the searchlight choice decoding analysis 100 times for each participant. In each repetition, we randomly sampled a subset of trials so that the number of trials associated with the left and right button presses was fully balanced across choices and runs. We then performed the same GLM and searchlight analysis as described above on a subset of data to obtain a decoding accuracy map per repetition, yielding a total of 100 accuracy maps per participant. The within-participant averaged accuracy maps were then forwarded to a group level t-test to identify brain regions which carry choice-related information. Importantly, by keeping the number of left and right button presses balanced across choices and runs, this analysis eliminated

potential confounds related to motor planning. If informative clusters reported in the main result were mainly driven by motor planning rather than by choices, we would not expect choice-related information in the reported regions. Reversely, a similar pattern of informative clusters would strengthen the result of the main analysis.

Results

Behavior

The overall behavioral performance of participants during the scanning session was highly accurate. The average accuracy rate was 0.881 (SD: 0.057; range: 0.778 - 0.99), while the average reaction time (latencies between the onsets of the target screens and button presses) was 0.554 (SD: 0.104, range: 0.359 - 0.77).

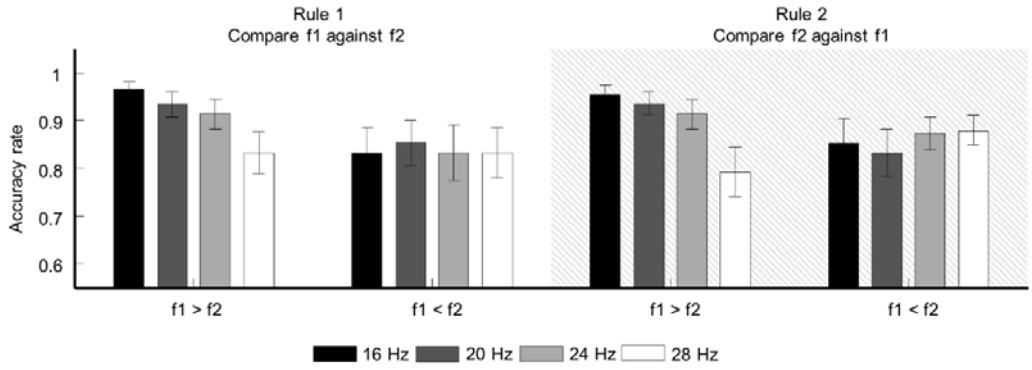

Fig. 2. Behavioral performance. The bar plots show the mean accuracy rates across participants over all runs for different stimulus orders, rules, and f1 magnitudes. Error bars represent 95% confidence intervals (CIs) of the means.

We further examined participants' behavioral accuracies and reaction times with three-way repeated measure ANOVAs with task rule (compare f1 against f2 vs f2 against f1), stimulus order (f1 > f2 vs f1 < f2), and f1 magnitude (16Hz, 20Hz, 24Hz, and 28Hz) as within-subject factors, respectively. For the behavioral accuracy, there

was no task rule effect observable ($F(1,26) = 1.66$, $p = 0.209$). The performance remained stable regardless of which particular rule was applied, suggesting that the cognitive demands were equivalent across rules. In addition, we observed a significant effect of stimulus order ($F(1,26) = 7.749$, $p = 0.001$), with a slightly better performance in f1 > f2 trials than in f1 < f2 trials ($mean_{f1>f2} = 0.911$, $mean_{f1<f2} = 0.851$, $CI_{95} = [0.0166\ 0.1035]$). Moreover, there was a significant interaction between stimulus order and f1 magnitude ($F(3, 78) = 11.239$, $p < 0.001$). As indicated by linear trend analyses, participants' performance decreased slightly with an increasing f1 in f1>f2 trials (slope = -0.0113, $p < 0.001$), while the performance was unaffected by f1 magnitude in f1 < f2 trials (slope = 0.003, $p = 0.233$). Contrary to the behavioral accuracy, we did not reveal any difference in reaction times between conditions.

Considering the possibility that response biases and the exclusion of incorrect trials from fMRI analysis may cause differences in stimulus order and motor response distribution between choices and thereby distort the outcome of the fMRI analysis, we performed Pearson chi-square tests on data included in the fMRI analysis, for each participant respectively. The tests did not reveal significant differences in the distribution of stimulus orders and motor responses between choices in any of the participants (all $p > 0.1$, uncorrected), suggesting that participants' choice behavior included in the fMRI analysis was not biased by the stimulus order or motor response.

In addition, the same decoding analysis routine as used for the fMRI data was performed to test whether the numbers of trials associated with different stimulus orders and motor responses were predictive of choices. As the results of one-sided, one-tailed Wilcoxon sign rank tests show, neither stimulus order nor motor response was predictive of choices (all $p > 0.05$, Holm corrected).

353 Collectively, there is no evidence from our behavioral analyses indicating that the
354 fMRI results reported below were confounded by the physical properties of the
355 stimulus order and selection of the ensuing motor responses.

356

357 **Neuroimaging results**

358 The main objective of the present study was to identify brain regions that carry
359 information about perceptual choice independent of the physical properties of
360 stimulus orders and selection of the ensuing manual responses. Using whole-brain
361 searchlight MVPA, we tested for brain regions exhibiting distinguishable local activity
362 patterns between choices during the 2 s decision phase. The result of the whole-
363 brain searchlight analysis is shown in Fig. 3 (displayed at $p < 0.05$, FDR corrected for
364 multiple comparisons at the cluster level with a cluster-defining voxel-wise threshold
365 of $p < 0.001$). We were able to decode perceptual choices from the intraparietal
366 sulcus (IPS, mainly in area hIP3; cluster size = 130, peak voxel: [-34 -52 50], $t_{[26]}$ =
367 5.115, mean decoding accuracy at the peak = 57.737%, CI_{95} = [4.628% 10.847%])
368 and the dorsal premotor cortex (PMd, BA 6) in the left hemisphere, contralateral
369 hemisphere to the response effector (cluster size = 109, peak voxel: [-20 2 70], $t_{[26]}$ =
370 4.864, mean decoding accuracy = 60.504%, CI_{95} = [6.066% 14.943%). To test
371 whether choices are indeed represented in a lateralized manner, we conducted two-
372 sided paired t-tests between decoding accuracies extracted from the identified peak
373 voxels and those extracted from the corresponding locations in the right hemisphere
374 (right panel in Fig. 3). These tests show that decoding accuracies extracted from the
375 identified peak voxels were significantly higher than those in the right hemisphere,
376 ipsilateral to the response effector (IPS: $t_{[26]}$ = 2.413, $p = 0.002$, CI_{95} = [0.928%

11.619%]; PMd: $t_{[26]}$ = 4.43, p < 0.001, CI_{95} = [7.137% 19.467%]), corroborating the lateralized representation of choice-related information.

We were further interested in whether decoding accuracies in the reported regions were explanatory to the behavioral performance. To this end, we estimated the Pearson correlation between the decoding accuracy and behavioral performance. We were not able to find statistical evidence for such a linkage between them in any of the reported regions (IPS: rho = 0.089, p = 0.659; PMd: rho = -0.016, p = 0.938).

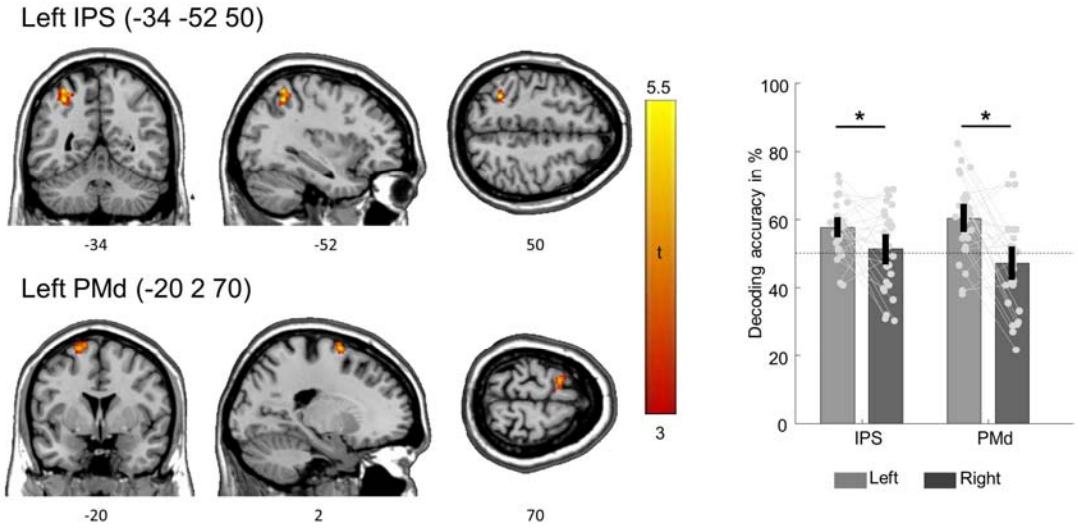

Fig. 3. fMRI decoding results**.** The left IPS and the PMd were found to carry choice-related information independent of stimulus order and ensuing button press, contralateral to the response effector (P_{FDR} < 0.05, cluster corrected for multiple comparisons). Coordinates refer to MNI space and indicate the peak voxel of each region respectively. The unthresholded statistical map can be inspected at https://www.neurovault.org/images/256861/ The bar plot shows decoding accuracies at the reported peak voxels and at the equivalent positions in the right hemisphere, ipsilateral to the response effector. Error bars represent 95% CIs of the means, while dots indicate individual participants' decoding accuracies in each brain region. Asterisks indicate statistically significant differences between hemispheres at p < 0.05, Holm corrected for multiple comparisons. Participant-specific decoding accuracy maps are available at https://doi.org/10.6084/m9.figshare.9920111.v2

Importantly, the pattern of informative clusters at the group level remains similar across different searchlight radiuses. We performed the same MVPA with searchlight radii of 3-5 voxels and found that locations of significant informative clusters remain centered in the left IPS and PMd (Fig. 4). Moreover, results of two-sided paired t-

401 tests between all possible pairs show that decoding accuracies do not differ across
402 searchlight radii (all $p > 0.05$, Holm corrected).

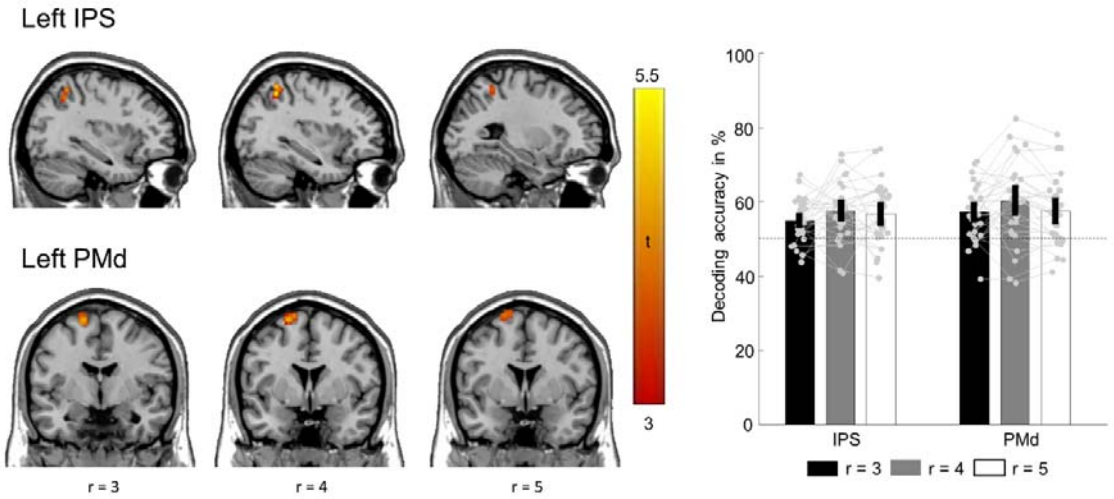

403
404 **Fig. 4.** fMRI decoding results using three different searchlight radii. The left panel depicts the
405 informative clusters (one column for each radius, indicated by r). Bar plot in the right panel displays
406 decoding accuracies at peak voxels of the IPS and PMd clusters for each radius respectively. The
407 unthresholded statistical maps are available at https://www.neurovault.org/collections/5936/ Error bars
408 indicate 95% CIs of the means. Grey dots and lines represent individual participants' decoding
409 accuracies.
410

411 We performed an additional decoding analysis to explore whether the identified brain
412 regions with significant above-chance decoding accuracies may result from a bias
413 toward a particular choice-response association. We repeated the searchlight choice
414 decoding analysis and eliminated the potential motor-related confound by keeping
415 the left and right button presses balanced across choices and runs. This analysis
416 yielded a highly similar pattern of brain regions carrying choice-related information as
417 in the main analysis. As shown in Fig. 5 (reported at $p < 0.001$ uncorrected due to
418 significant reduced amount of data compared to the main analysis), choice-related
419 information was again found in the left IPS ([-34 -52 52], $t_{[26]} = 5.173$, cluster size =
420 128, mean = 56.157%, CI_{95} = [3.711% 8.603%) and in the left PMd ([-20 0 72], $t_{[26]}$ =
421 4.443, cluster size = 76, mean = 57.662%; CI_{95} = [4.117% 11.207%]). Altogether, the

422 results of both behavioral and neuroimaging control analyses suggest that the main
423 results were not driven by motor-related confounds.

424

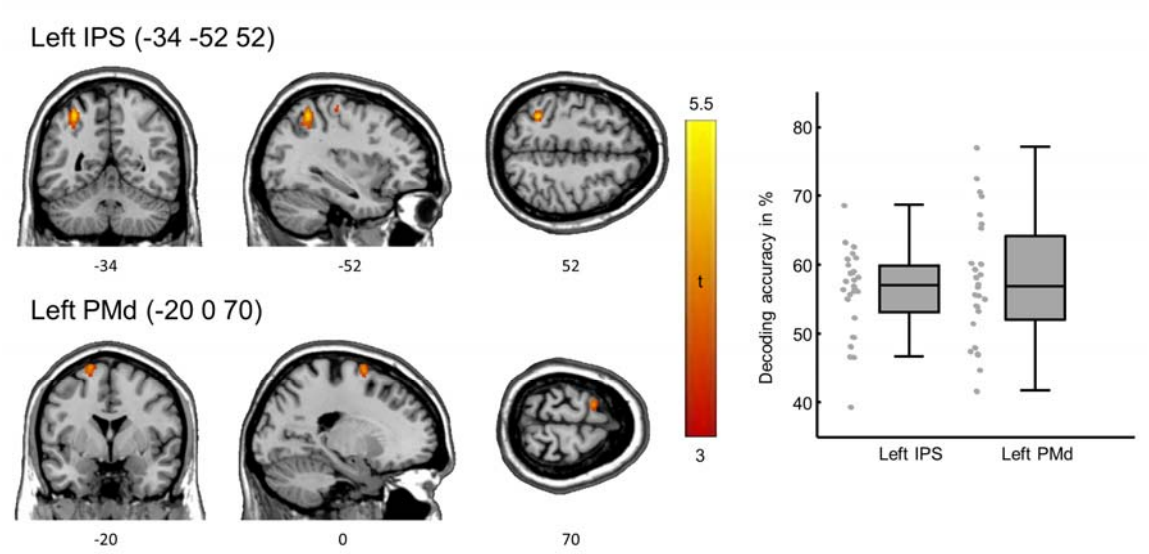

425
426 **Fig 5.** fMRI control analysis result. The left panel displays significant clusters detected by the analysis
427 controlling for motor-related confounds (displayed at $p < 0.001$, uncorrected). The unthresholded
428 statistical map is available at https://www.neurovault.org/images/256864/ The right panel shows box
429 plots for IPS and PMd separately. Box edges indicate the 25th and 75th percentiles, central horizontal
430 lines correspond to the median. Grey dots represent individual participants' decoding accuracies.

431

432 Next, we compared the result of the present study with that of our previous study, in
433 which decisions were communicated with saccades, instead of button presses (Wu et
434 al., 2019, n = 30). Similar to the present study, choice-selective activity was found in
435 premotor and intraparietal regions, with the difference that it was evident in both
436 hemispheres. The previous study also reported choice-selective activity in the left
437 prefrontal cortex (PFC), while it was absent in the current study. Notably, although
438 both studies identified premotor and intraparietal regions as carrying choice-related
439 information, there were no overlapping clusters. In particular, the premotor clusters
440 identified in the previous study were located in the junction of precentral gyri and the
441 caudal-most part of the superior frontal sulci ($peak_{left}$: [-32 10 62], $peak_{right}$: [34 4 52]),

commonly referred to as the FEF (determined with the probabilistic maps by Wang et al., 2015; www.princeton.edu/~napl\vtpm.htm). In contrast, the premotor cluster detected in the current study lies in the adjacent PMd (-20 0 72), dorsocaudal to the FEF (determined with the SPM Anatomy toolbox version 3; Eickhoff et al., 2005), hinting that the location of choice-related information might shift between regions specialized for eye and hand movements depending on what response effector is used.

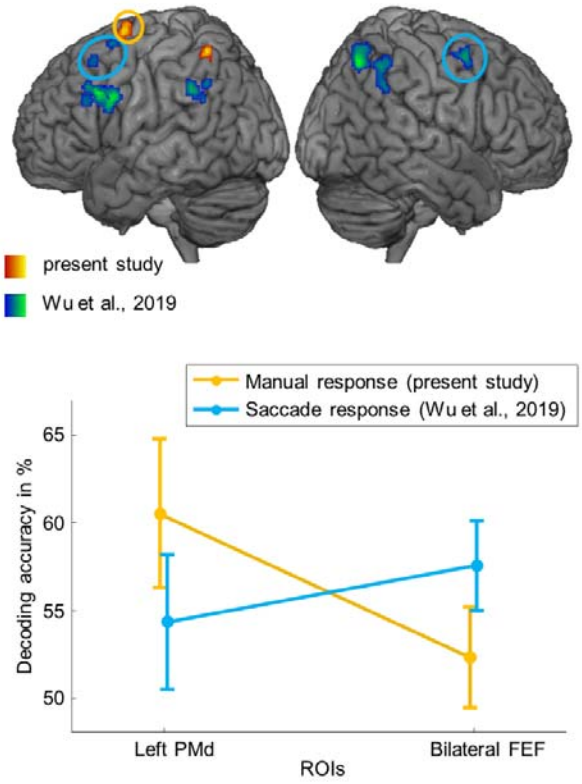

Fig.6. Comparison with results from the saccade version of the task (Wu et al., 2019, n = 30). The upper panel displays brain regions carrying choice-related information as identified in the present study (in red-orange) and those detected in our previous work using saccades as decision reports (in blue-green, unthresholded statistical map available at https://www.neurovault.org/images/63793/), both displayed at $p_{FDR} < 0.05$, cluster corrected. The circles indicate the premotor and intraparietal clusters used for ROI analysis. The lower panel depicts mean decoding accuracies across participants collapsed across response modalities and effector-specific regions. Error bars indicate 95% CIs of the means.

To further assess this possibility, we ran a set of regions of interest (ROI) analyses. First, we took the peak voxels in the bilateral FEF from the previous study as the ROI

for the current data. For each participant, we extracted decoding accuracies from these voxels and averaged them. The averaged decoding accuracies were then submitted to a two-tailed, one-sample t-test against the chance level. Likewise, we used the peak voxel of the PMd cluster from the present study as the ROI for the previous study and tested whether choices could be reliably decoded from the PMd. The results of these ROI analyses support the interpretation of an effector-dependent shift of choice representation within the premotor cortex (Fig. 6). Despite the higher sensitivity of ROI approach, the mean decoding accuracy computed from the bilateral FEF in the present study did not surpass the chance level ($t_{[26]}$ = 1.534, mean = 52.272%; CI_{95} = [-0.772% 5.315%], p = 0.137). Likewise, the mean decoding accuracy in the left PMd derived from the previous study did not differ significantly from the chance level ($t_{[29]}$ = 2.172, mean = 54.301%; CI_{95} = [0.250% 8.352%], p = 0.076, Holm corrected). That is, when manual response was used, choice could only be reliably decoded from the left PMd, but not from the FEF. Conversely, choice could only be read out from the FEF, but not from the PMd, when saccadic response was required (Fig. 6).

Discussion

In the present study, we sought to identify human brain regions that represent abstract choices in the context of vibrotactile frequency comparisons. We used fMRI combined with a variant of the vibrotactile frequency discrimination task which allowed us to dissociate choice-selective BOLD signals from those related to the physical properties of stimulus orders and the selection of manual responses. We identified the left IPS and PMd, contralateral to the response effector, as carrying choice-related information. Notably, using the same task, but saccades as response

effector, our previous study (Wu et al., 2019) also reported choice-related information in intraparietal and premotor regions. Interestingly, the informative premotor cluster was centered in the FEF rather than in the PMd. Evidence from these two studies suggests a response modality-specific organization of abstract choice representations in the context of vibrotactile comparisons.

The pivotal role of the premotor cortex in decision formation during vibrotactile comparisons has been established by the seminal work of Romo and colleagues using neurophysiological recordings in monkeys (reviewed in Romo and de Lafuente, 2013). The premotor cortex is strongly implicated in the computation of comparisons between the two sequentially presented stimuli, based on the consistent observation of choice-predictive signals before the initiation of manual responses (Hernández et al., 2002; 2010). In line with these reports, we identified the dorsal part of the premotor cortex as carrying choice-related information, with the crucial difference that choices in the present study were independent of sensorimotor components, while choices in the above-mentioned monkey neurophysiological studies were inextricably linked with them. Taking this into account, the finding of such abstract choice representations in a region that is primarily associated with the planning and preparation of manual actions may not appear straightforward. Indeed, results from few human fMRI studies in the visual domain, wherein perceptual choices were disentangled from specific actions, are inconsistent. On the one hand, several studies failed to find evidence for decision-related BOLD signals in the premotor cortex when choices were decoupled from actions (e.g., Hebart et al., 2012; Filimon et al., 2013). On the other hand, premotor activity reflecting categorical choices regarding the stimulus identity independent of motor planning has been shown in other human fMRI studies (e.g., Hebart et al., 2014). With this study, we provide

511 additional fMRI evidence for a premotor involvement in the representation of choices
512 in a more abstract, internal cognitive format.

513 Hereof, it is important to note that the analysis we used in the present study does not
514 permit an inference about whether abstract choices are indeed encoded in the PMd
515 or generated elsewhere. Independent of this issue, one possible explanation for our
516 premotor finding is that the PMd serves as a node for short-term storage of abstract
517 choice representations and the transformation into commands for concrete manual
518 movement once all information required for the execution of specific actions are
519 known. This interpretation agrees with a recent study showing a causal role of the
520 premotor cortex in the flexible stimulus-response mapping in mice (Wu Z. et al., 2019)
521 and monkey neurophysiological studies implicating the PMd in the retrieval and
522 integration of task-relevant information necessary for specification of particular
523 actions (e.g., Nakayama et al., 2008; Yamagata, 2009, 2012).

524 While there is a vast amount of neurophysiological evidence for the premotor
525 involvement during vibrotactile comparisons, neural activities in the posterior parietal
526 cortex (PPC) has remained largely unexplored in this context. Nevertheless, our
527 finding of intraparietal choice representation was not surprising. Similar to the
528 premotor area, posterior parietal regions are thought to be crucially involved in
529 various decision-making tasks, most prominently when decisions are communicated
530 by saccades (Gold & Shadlen, 2007). In particular, activity in the monkey LIP
531 (homologous to the intraparietal subregions in humans) has been shown to mimic the
532 presumed evidence accumulation toward one or the other saccade choices and
533 thereupon regarded as the explicit neural representation of the evolving decisions
534 (Shadlen & Kiani, 2013, but see Huk et al., 2017 for a critical review). Moreover,
535 evidence from recent studies on a wide range of decision-making tasks suggests that

PPC's involvement is not confined to motor decisions but pertains to decisions at different levels of abstraction. For instance, both monkey and human PPC have been shown to represent choices that were independent of the planning of saccade responses (Bennur & Gold, 2011; Hebart et al., 2012). Among studies in the broader context of decision making, findings from monkey neurophysiological recordings using visual categorization tasks are particular revealing (reviewed in Freedman & Assad, 2016). In these studies, monkeys were trained to perform delayed match-to-category tasks in which they decide whether the motion direction of the sample stimulus and the test stimulus belong to the same category based on a previously learned, arbitrarily defined boundary. After the test stimulus, monkeys indicated their decision on a match or mismatch with manual or saccadic responses. Using this task, LIP has been shown to exhibit signals reflecting the categorical choice which cannot be attributed to specific sensory stimulus properties nor action selection (Freedman & Assad, 2006; Swaminathan & Freedman, 2012; Swaminathan et al., 2013). Such categorical information is reminiscent of the choice-related information observed in our study as both are dissociated from sensory and motor components of the task and are thus, represented at a similar level of abstraction. The similarity between them opens the possibility of a common mechanism and thereby boosts the notion of the PPC, and IPS more specifically, as a central node mediating abstract cognitive computations (Freedman & Assad, 2016).

Given the above-mentioned functions ascribed to the PPC, one question which naturally emerges from our results is whether the reported choice-related information is directly computed in the PPC via the evidence accumulation process or other mechanisms. We are not able to answer this question with our experimental design. In this study, we only used stimulus pairs with supra-threshold differences to facilitate

561 the decodability of choice-related information. This is, however, problematic for
562 assessing neural correlates of evidence accumulation as they would, according to
563 the accumulation-to-bound model (Ratcliff et al., 2016), provide strong momentary
564 evidence signals which are difficult to distinguish as such. Similar to the premotor
565 cortex, it is possible that the IPS merely receives choice-related signals from
566 elsewhere in the brain and thus, is not actively involved in the decision formation.
567 However, there is evidence from several lines of research that warrants the IPS
568 being a promising candidate region for decision formation during vibrotactile
569 comparisons.

570 First, vibrotactile comparisons as implemented in the present study can be regarded
571 as a process in which a choice is made based on the relation between two
572 magnitudes. Combined evidence from monkey neurophysiology and human
573 neuroimaging suggest that magnitudes and the relation between them are encoded
574 by a network comprising the IPS and lateral PFC (reviewed in Jakobs et al., 2013).
575 Moreover, the IPS appears to be the first region within this network to process
576 magnitude information (reviewed in Nieder, 2016). Second, Herding and colleagues
577 (2019) showed that the centro-parietal positivity (CPP) in EEG signal, which has
578 been suggested as a proxy for accumulated evidence across a variety of decision-
579 making tasks (O'Connell et al., 2012; Kelly & O'Connell, 2013), also indexes the
580 amount of sensory evidence during vibrotactile comparisons. More specifically, they
581 identified the left IPS as the likely source of the CPP component reflecting the signed
582 subjectively perceived difference between two frequencies. Notably, in this study,
583 participants always compared f2 against f1. It would be interesting to explore whether
584 and how this effect is modulated by comparisons in the reversed direction. Finally,
585 using a reversible inactivation approach to investigate PPC's contribution to sensory

586 evaluation and action selection. Zhou and Freedman (2019) revealed that monkeys'
587 decisions were more severely affected when visual stimuli, rather than motor targets,
588 were placed in the inactivated receptive fields of LIP neurons under investigation,
589 providing compelling evidence for the causal role of the PPC in the sensory aspect of
590 visual decisions. Given that the IPS is thought to have a similar role as a mediating
591 node in the sensorimotor transformation across multiple sensory domains, it is
592 intriguing to see whether a causal effect could also be demonstrated during
593 vibrotactile comparisons.

594 With the present finding of premotor and intraparietal choice-selectivity, we have also
595 replicated the finding of our previous study using the same task but with saccades as
596 the response modality (Wu et al., 2019). When comparing both studies more closely,
597 two differences are apparent. First, choice-related information was found in bilateral
598 premotor and intraparietal regions when saccades were used. However, when
599 manual responses were required, the premotor and intraparietal selectivity was only
600 evident in the contralateral hemisphere. Moreover, we observed a relocation of
601 choice-related information within the premotor area from the FEF to the PMd.
602 Importantly, we did not assign these functional labels merely based on the required
603 response modalities tasks. Both the FEF and the PMd were determined by means of
604 well-established functional probability maps. In addition, the spatial arrangement of
605 the FEF and the PMd clusters as identified by the spatially unbiased whole-brain
606 searchlight routines in these two studies corresponds well to that reported in
607 monkeys (e.g. Petrides, 1982; Halsband & Passingham, 1982; Bruce & Goldberg,
608 1985) and humans (Amiez, 2006), with saccade-related premotor region lying more
609 anterior and rostral to premotor region exhibiting activities related to manual
610 movements. Thus, it is unlikely that these differences were merely a by-product of

611 idiosyncratic differences between samples. Altogether, the results from these two
612 studies suggest a response modality-dependent organization of abstract choice
613 representations. One question emerged from this interpretation concerns whether the
614 posited response modality-dependent organization of abstract choice information is
615 confined to a specific level of abstraction. For instance, the dependency observed in
616 our studies might result from the explicit foreknowledge of the required response
617 modality. Evidence from other fMRI studies suggests that decision-related activities
618 may occur elsewhere when the required response modality is not known (Ho et al.,
619 2009; Liu and Pleskac, 2011; Filimon et al., 2013). In this light, future studies
620 combining the present task with a wide range of response modalities, target locations,
621 and task difficulties will provide essential insights into how vibrotactile choices are
622 evolved and transformed into internal cognitive states in humans.

623

624 ## Acknowledgements

625 This research was supported by the Deutsche Forschungsgemeinschaft (DFG) –
626 project number 409180874. We thank Pia Schröder for many inspiring discussions
627 and Sam Gijsen for proof reading the article.

628

629 ## Author contributions

630 Y.W. and F.B. designed the experiment and interpreted the results. Y.W. and L.A.V.
631 conducted the experiment, Y.W. analyzed the data and wrote the manuscript. L.A.V.
632 and F.B. reviewed and edited the manuscript.

633

Competing interests

The authors declare no competing financial interests.

References

Amiez, C., Kostopoulos, P., Champod, A., Petrides, M., 2006. Local Morphology Predicts Functional Organization of the Dorsal Premotor Region in the Human Brain. J. Neurosci. 26, 2724–2731. https://doi.org/10.1523/JNEUROSCI.4739-05.2006

Behzadi, Y., Restom, K., Liau, J., Liu, T.T., 2007. A component based noise correction method (CompCor) for BOLD and perfusion based fMRI. Neuroimage 37, 90–101. https://doi.org/10.1016/j.neuroimage.2007.04.042

Bennur, S., Gold, J.I., 2011. Distinct Representations of a Perceptual Decision and the Associated Oculomotor Plan in the Monkey Lateral Intraparietal Area. J. Neurosci. 31, 913–921. https://doi.org/10.1523/JNEUROSCI.4417-10.2011

Brainard, D.H., 1997. The Psychophysics Toolbox. Spat. Vis. 10, 433—436. https://doi.org/10.1163/156856897x00357

Bruce, C.J., Goldberg, M.E., 1985. Primate frontal eye fields. I. Single neurons discharging before saccades. J. Neurophysiol. 53, 603–635. https://doi.org/10.1152/jn.1985.53.3.603

Chang, C.-C., Lin, C.-J., 2011. LIBSVM. ACM Trans. Intell. Syst. Technol. 2, 1–27. https://doi.org/10.1145/1961189.1961199

Cisek, P., Kalaska, J.F., 2010. Neural mechanisms for interacting with a world full of action choices. Annu. Rev. Neurosci. 33, 269–98. https://doi.org/10.1146/annurev.neuro.051508.135409

Ding, L., Gold, J.I., 2012. Neural Correlates of Perceptual Decision Making before, during, and after Decision Commitment in Monkey Frontal Eye Field. Cereb. Cortex 22, 1052–1067. https://doi.org/10.1093/cercor/bhr178

Eickhoff, S.B., Stephan, K.E., Mohlberg, H., Grefkes, C., Fink, G.R., Amunts, K., Zilles, K., 2005. A new SPM toolbox for combining probabilistic cytoarchitectonic maps and functional imaging data. Neuroimage 25, 1325–35. https://doi.org/10.1016/j.neuroimage.2004.12.034

Freedman, D.J., Assad, J.A., 2006. Experience-dependent representation of visual categories in parietal cortex. Nature 443, 85–88. https://doi.org/10.1038/nature05078

668 Filimon, F., Philiastides, M.G., Nelson, J.D., Kloosterman, N.A., Heekeren, H.R.,
669 2013. How Embodied Is Perceptual Decision Making ? Evidence for Separate
670 Processing of Perceptual and Motor Decisions. J. Neurosci. 33, 2121–2136.
671 https://doi.org/10.1523/JNEUROSCI.2334-12.2013

672 Freedman, D.J., Assad, J.A., 2016. Neuronal Mechanisms of Visual Categorization:
673 An Abstract View on Decision Making. Annu. Rev. Neurosci. 39, 129–147.
674 https://doi.org/10.1146/annurev-neuro-071714-033919

675 Gold, J.I., Shadlen, M.N., 2007. The Neural Basis of Decision Making. Annu. Rev.
676 Neurosci. 30, 535–574.
677 https://doi.org/10.1146/annurev.neuro.29.051605.113038

678 Görgen, K., Hebart, M.N., Allefeld, C., Haynes, J.-D., 2017. The Same Analysis
679 Approach: Practical protection against the pitfalls of novel neuroimaging analysis
680 methods 1–12. https://doi.org/10.1016/j.neuroimage.2017.12.083

681 Halsband, U., Passingham, R., 1982. The role of premotor and parietal cortex in the
682 direction of action. Brain Res. 240, 368–372. https://doi.org/10.1016/0006-
683 8993(82)90239-6

684 Hebart, M.N., Baker, C.I., 2017. Deconstructing multivariate decoding for the study of
685 brain function. Neuroimage 1–15.
686 https://doi.org/10.1016/j.neuroimage.2017.08.005

687 Hebart, M.N., Donner, T.H., Haynes, J.D., 2012. Human visual and parietal cortex
688 encode visual choices independent of motor plans. Neuroimage 63, 1393–1403.
689 https://doi.org/10.1016/j.neuroimage.2012.08.027

690 Hebart, M.N., Goergen, K., Haynes, J.-D., 2015. The Decoding Toolbox (TDT): a
691 versatile software package for multivariate analyses of functional imaging data.
692 Front. Neuroinform. 8, 1–18. https://doi.org/10.3389/fninf.2014.00088

693 Hebart, M.N., Schriever, Y., Donner, T.H., Haynes, J.-D., 2014. The Relationship
694 between Perceptual Decision Variables and Confidence in the Human Brain.
695 Cereb. Cortex bhu181-. https://doi.org/10.1093/cercor/bhu181

696 Herding, J., Ludwig, S., Blankenburg, F., 2017. Response-Modality-Specific
697 Encoding of Human Choices in Upper Beta Band Oscillations during Vibrotactile
698 Comparisons. Front. Hum. Neurosci. 11, 1:11.
699 https://doi.org/10.3389/fnhum.2017.00118

700 Herding, J., Spitzer, B., Blankenburg, F., 2016. Upper Beta Band Oscillations in
701 Human Premotor Cortex Encode Subjective Choices in a Vibrotactile
702 Comparison Task. J. Cogn. Neurosci. 28, 668–679.
703 https://doi.org/10.1162/jocn_a_00932

704 Hernández, A., Nácher, V., Luna, R., Zainos, A., Lemus, L., Alvarez, M., Vázquez, Y.,
705 Camarillo, L., Romo, R., 2010. Decoding a perceptual decision process across
706 cortex. Neuron 66, 300–14. https://doi.org/10.1016/j.neuron.2010.03.031

Hernández, A., Zainos, A., Romo, R., 2002. Temporal Evolution of a Decision-Making Process in Medial Premotor Cortex 33, 959–972.

Ho, T.C., Brown, S., Serences, J.T., 2009. Domain General Mechanisms of Perceptual Decision Making in Human Cortex. J. Neurosci. 29, 8675–8687. https://doi.org/10.1523/JNEUROSCI.5984-08.2009

Horwitz, G.D., Newsome, W.T., 1999. Separate Signals for Target Selection and Movement Specification in the Superior Colliculus. Science. 284, 1158–1161. https://doi.org/10.1126/science.284.5417.1158

Huk, A.C., Katz, L.N., Yates, J.L., 2017. The Role of the Lateral Intraparietal Area in (the Study of) Decision Making. Annu. Rev. Neurosci. 40, 349–372. https://doi.org/10.1146/annurev-neuro-072116-031508

Jacob, S.N., Vallentin, D., Nieder, A., 2012. Relating magnitudes: the brain's code for proportions. Trends Cogn. Sci. 16, 157–166. https://doi.org/10.1016/J.TICS.2012.02.002

Kelly, S.P., O'Connell, R.G., 2013. Internal and External Influences on the Rate of Sensory Evidence Accumulation in the Human Brain. J. Neurosci. 33, 19434 LP-19441. https://doi.org/10.1523/JNEUROSCI.3355-13.2013

Kim, J.-N., Shadlen, M.N., 1999. Neural correlates of a decision in the dorsolateral prefrontal cortex of the macaque. Nat. Neurosci. 2, 176–185. https://doi.org/10.1038/5739

Kriegeskorte, N., Goebel, R., Bandettini, P.A., 2006. Information-based functional brain mapping. Proc. Natl. Acad. Sci. U. S. A. 103, 3863–8. https://doi.org/10.1073/pnas.0600244103

Liu, T., Pleskac, T.J., 2011. Neural correlates of evidence accumulation in a perceptual decision task. J. Neurophysiol. 48824, 2383–2398. https://doi.org/10.1152/jn.00413.2011.

Nakayama, Y., Yamagata, T., Tanji, J., Hoshi, E., 2008. Transformation of a virtual action plan into a motor plan in the premotor cortex. J. Neurosci. 28, 10287–97. https://doi.org/10.1523/JNEUROSCI.2372-08.2008

Nieder, A., 2016. The neuronal code for number. Nat. Rev. Neurosci. 17, 366–82. https://doi.org/10.1038/nrn.2016.40

Park, I.M., Meister, M.L.R., Huk, A.C., Pillow, J.W., 2014. Encoding and decoding in parietal cortex during sensorimotor decision-making. Nat. Neurosci. 17, 1395–403. https://doi.org/10.1038/nn.3800

O'Connell, R.G., Dockree, P.M., Kelly, S.P., 2012. A supramodal accumulation-to-bound signal that determines perceptual decisions in humans. Nat. Neurosci. 15, 1729.

744 Petrides, M., 1982. Motor conditional associative-learning after selective prefrontal
745 lesions in the monkey. Behav. Brain Res. 5, 407–413.
746 https://doi.org/10.1016/0166-4328(82)90044-4

747 Ratcliff, R., Cherian, A., Segraves, M., 2003. A Comparison of Macaque Behavior
748 and Superior Colliculus Neuronal Activity to Predictions From Models of Two-
749 Choice Decisions. J. Neurophysiol. 90, 1392–1407.
750 https://doi.org/10.1152/jn.01049.2002

751 Ratcliff, R., Smith, P.L., Brown, S.D., McKoon, G., 2016. Diffusion Decision Model:
752 Current Issues and History. Trends Cogn. Sci. 20, 260–281.
753 https://doi.org/10.1016/j.tics.2016.01.007

754 Roitman, J.D., Shadlen, M.N., 2002. Response of neurons in the lateral intraparietal
755 area during a combined visual discrimination reaction time task. J. Neurosci. 22,
756 9475–89. https://doi.org/10.1523/JNEUROSCI.22-21-09475.2002

757 Romo, R., de Lafuente, V., 2013. Conversion of sensory signals into perceptual
758 decisions. Prog. Neurobiol. 103, 41–75.
759 https://doi.org/10.1016/j.pneurobio.2012.03.007

760 Romo, R., Hernández, A., Zainos, A., 2004. Neuronal Correlates of a Perceptual
761 Decision in Ventral Premotor Cortex. Neuron 41, 165–173.
762 https://doi.org/10.1016/S0896-6273(03)00817-1

763 Shadlen, M.N.N., Kiani, R., 2013. Decision making as a window on cognition. Neuron
764 80, 791–806. https://doi.org/10.1016/j.neuron.2013.10.047

765 Shadlen, M.N., Newsome, W.T., 2001. Neural Basis of a Perceptual Decision in the
766 Parietal Cortex (Area LIP) of the Rhesus Monkey. J. Neurophysiol. 86, 1916–
767 1936. https://doi.org/10.1152/jn.2001.86.4.1916

768 Swaminathan, S.K., Freedman, D.J., 2012. Preferential encoding of visual categories
769 in parietal cortex compared with prefrontal cortex. Nat. Neurosci. 15, 315–320.
770 https://doi.org/10.1038/nn.3016

771 Swaminathan, S.K., Masse, N.Y., Freedman, D.J., 2013. A Comparison of Lateral
772 and Medial Intraparietal Areas during a Visual Categorization Task. J. Neurosci.
773 33, 13157 LP-13170. https://doi.org/10.1523/JNEUROSCI.5723-12.2013

774 Wang, L., Mruczek, R.E.B., Arcaro, M.J., Kastner, S., 2015. Probabilistic Maps of
775 Visual Topography in Human Cortex. Cereb. Cortex 25, 3911–3931.
776 https://doi.org/10.1093/cercor/bhu277

777 Wu, Z., Litwin-Kumar, A., Shamash, P., Taylor, A., Axel, R., Shadlen, M., 2019a
778 Context-Dependent Decision Making in a Premotor Circuit (September 17, 2019).
779 CELL-D-19-02522. Available at SSRN: https://ssrn.com/abstract=3455473

780 Wu, Y-h., Velenosi, L.A., Schröder, P., Ludwig, S., Blankenburg, F., 2019b. Decoding
781 vibrotactile choice independent of stimulus order and saccade selection during

782 sequential comparisons. Hum. Brain Mapp. 1898–1907.
783 https://doi.org/10.1002/hbm.24499

784 Yamagata, T., Nakayama, Y., Tanji, J., Hoshi, E., 2009. Processing of visual signals
785 for direct specification of motor targets and for conceptual representation of
786 action targets in the dorsal and ventral premotor cortex. J. Neurophysiol. 102,
787 3280–94. https://doi.org/10.1152/jn.00452.2009

788 Yamagata, T., Nakayama, Y., Tanji, J., Hoshi, E., 2012. Distinct information
789 representation and processing for goal-directed behavior in the dorsolateral and
790 ventrolateral prefrontal cortex and the dorsal premotor cortex. J. Neurosci. 32,
791 12934–49. https://doi.org/10.1523/JNEUROSCI.2398-12.2012

792 Zhou, Y., Freedman, D.J., 2019. Posterior parietal cortex plays a causal role in
793 perceptual and categorical decisions. Science (80-.). 365, 180 LP-185.
794 https://doi.org/10.1126/science.aaw8347

795